DESIGN ANALYSIS OF A FRICTION DISK ROTOR

By

DIXON KEITH FOSS

Bachelor of Science

Oklahoma State University

1962

Submitted to the faculty of the Graduate School of
the Oklahoma State University
in partial fulfillment of the requirements
for the degree of
MASTER OF SCIENCE
August, 1964

DESIGN ANALYSIS OF A FRICTION DISK ROTOR

Thesis Approved:

Gerald D. Parker

Glen W. Zumwalt

Dean of the Graduate School

TABLE OF CONTENTS

LIST OF TABLES

LIST OF FIGURES

LIST OF SYMBOLS

d	1/2 Disk Spacing
η	Rotor Efficiency
HP	Horsepower
M	Torque
n	Number of Disks
P	Pressure
Q	Volume Flow Rate
ρ	Fluid Density
r	Radial Distance
S	Disk Spacing
U (or u)	Radial Velocity
U_o (or u_o)	Radial Velocity at Inlet
v	Tangential Velocity
V	Relative Tangential Velocity
ν	Fluid Kinematic Viscosity
W	Axial Velocity
ω	Angular Velocity of Disks
X	Radial Distance, Transformed Co-ordinates
Y	Axial Distance, Transformed Co-ordinates
Z	Axial Distance

SUBSCRIPTS

i	Condition at Disk Port Radius
e	Condition at Outer Disk Radius
-	Superscript, Dimensionless Variable
s	Static Condition
d	Dynamic Condition

CHAPTER I

INTRODUCTION

The purpose of this investigation is to obtain design information on a friction disk rotor. At the present time there is no information from which a rotor of this type can be easily designed to deliver a given quantity of air at a given pressure. A knowledge of the design requirements of the rotor would lead directly to the design of a complete fan unit. The complete fan consists of the rotor and the housing, which includes the inlet and diffuser sections. Because the housing design would be similar to that of any centrifugal fan this subject has not been covered in this study. Information pertaining to efficient housing design is readily available; two sources have been cited [3], [11][1].

Although this study has been limited to the use of air as the working fluid any other fluid could be used by substituting the appropriate values of density and viscosity.

This study includes the results of a mathematical solution by Pohlhausen and Breiter [2], from which the performance characteristics are derived. An experimental fan was built and tested in order to compare the characteristics of a practical design with those of the ideal model in the mathematical analysis.

---

[1]Numbers in brackets designate references at end of paper.

The report is concluded with a summary of the results and an outline of design methods. The outline includes specifications of all the critical dimensions of the rotor from given flow conditions and fluid properties.

General Statement of the Problem

A friction disk rotor differs from conventional vane type rotors in its manner of energy transfer. Just as the name implies, viscous friction is the sole means of energy exchange.

In order to explain the method in which viscous friction is employed let us consider a flat plate which is being moved through a fluid medium. The particles of fluid on the solid surface will move with the velocity of the plate as required by the condition of zero velocity at a solid boundary. The velocity gradient between these particles and the adjacent fluid layer will create a shear force which will accelerate the fluid. The net result of this shearing action between adjacent fluid layers is an acceleration of the fluid mass in the direction of motion of the plate. The amount of acceleration depends upon the velocity gradient so that fluid layers more distant from the plate will be affected less by the motion.

It can be seen that some of the energy required to move the plate through the fluid appears as kinetic energy in the fluid particles near the plate. Thus the motion of the plate exerts a pumping action on the fluid due to the viscous shearing forces between adjacent layers of the fluid.

The pumping action can be realized in a practical case if the plate is considered to be a series of disks mounted on a rotating

shaft and separated by small gaps. The fluid in the gap between each disk will be accelerated in the tangential direction by the shearing forces in the fluid. The rotation of the fluid about the axis of the shaft will result in an outward radial acceleration. If the fluid is allowed to enter through ports in the disk near the shaft a radial flow will exist. The pressure developed by the pump will depend upon the radial acceleration which is obviously a function of the tangential velocity.

An important point now arises which affects the efficiency of any machine operating on the friction disk principle. The radial velocity which exists due to an outward radial flow of fluid between the disks is also subject to the condition of zero velocity at the solid boundary. This condition now represents a loss of energy. The shearing forces retard the flow of fluid in the radial direction and produce a radial force in the disk. This force is the same at all points equidistant from the center of the disk so that it appears only as an internal force in the disk. Thus the efficiency of the friction disk pump will depend upon its ability to accelerate the fluid to a high tangential velocity and will be limited by the amount of energy which is lost as the fluid flows in the radial direction. Thus it appears that the efficiency will decrease as the radial velocity increases.

History

The friction disk principle was first used by Nikola Tesla in 1905. He received patents on a pump and a turbine which utilized the principle (Figs. 1 and 2) in 1913.

Most of his work was directed toward development of a steam

Fig. 1

N. TESLA.

FLUID PROPULSION.

APPLICATION FILED OCT. 21, 1909.

1,061,142. Patented May 6, 1913.

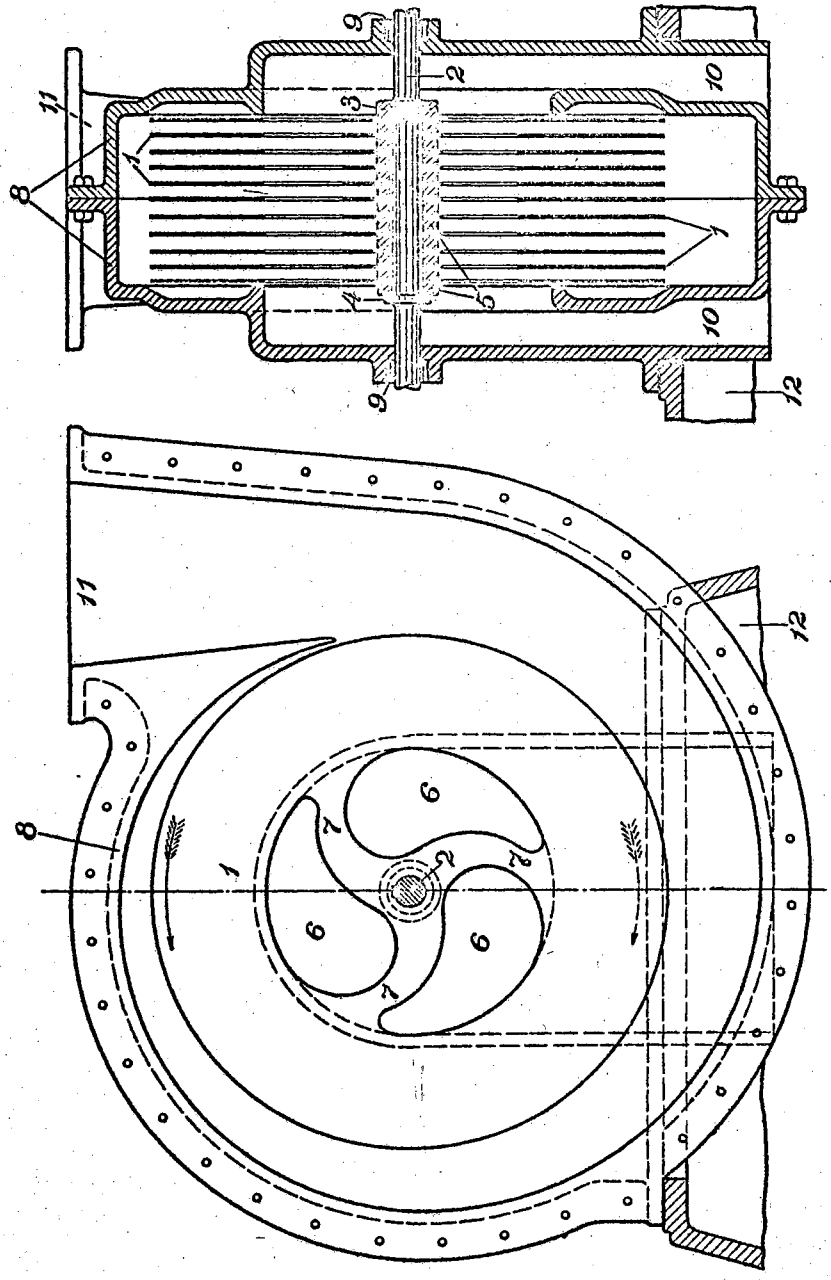

Witnesses:
R. Diaz Benitage
S. J. Dunham

Nikola Tesla,
Inventor

By his Attorneys
Kerr, Page, Cooper & Hayward

Fig. 2

N. TESLA.

TURBINE.

APPLICATION FILED JAN. 17, 1911.

1,061,206. Patented May 6, 1913.

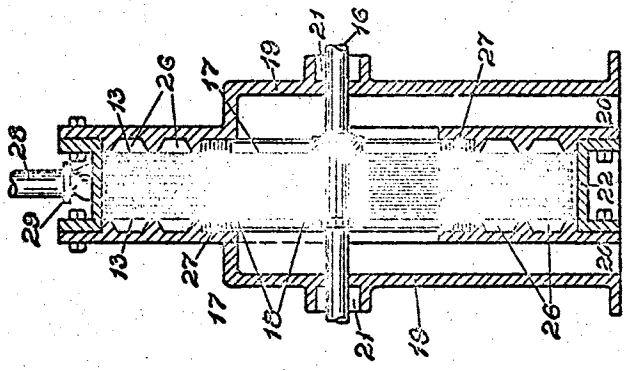

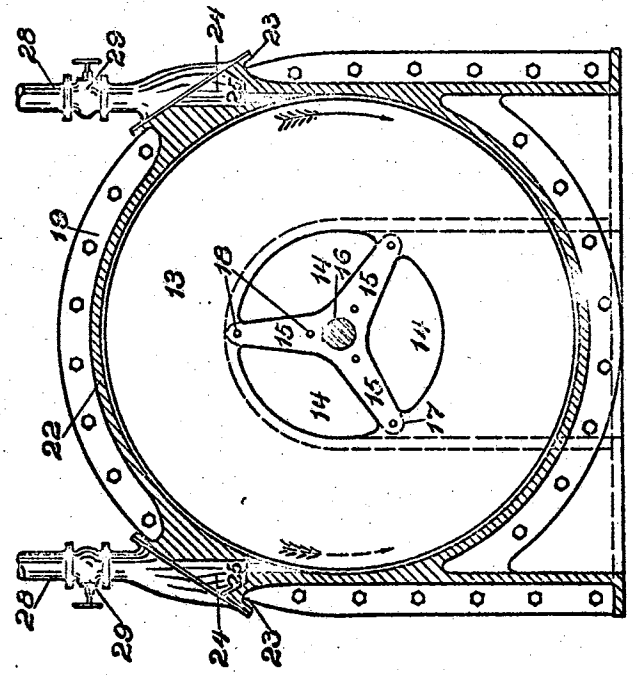

Witnesses:
R. Diaz Buitrago
Wm. Kohleber

Nikola Tesla, Inventor

By his Attorneys
Kerr Page Cooper & Hayward

turbine which could be used to drive the electric generators in the power plants which were being built during the early 1900's. The new turbine was designed to eliminate the complicated and precision construction required by the conventional impulse-reaction turbines.

The turbine developed by Tesla employed saturated steam as the working fluid. The steam was expanded to a high velocity through the inlet nozzle and entered tangentially into the space between the outer edges of the disks. In order to escape it had to move radially to the center of the disks where the exhaust ports were located. The high inlet velocity produced a steep velocity gradient and thus a high shearing stress at the disk surface. This high shearing stress over the surface of a series of disks produced a significant torque on the shaft.

One turbine built by Tesla consisted of 25 disks, 18 inches in diameter, the assembled unit occupied a space of 2 by 3 feet on the floor and stood 5 feet high. Saturated steam was admitted at 125 psig. and exhausted into the atmosphere. At 9000 RPM the turbine produced 200 HP with a thermal efficiency of about 50 percent. With the addition of superheat and a high vacuum condenser Tesla claimed this efficiency could be increased to over 80 percent. The Tesla turbine possessed several distinct advantages over the conventional design. Its versatility was increased by its ability to be reversed easily. This was done by merely adding another nozzle which acts in the opposite direction from the first.

Several companies negotiated with Tesla in an attempt to support his investigation, but Tesla refused their aid and was unwilling to release any of the information from his tests. Because of this he

lost much of his financial backing and was forced to discontinue his tests in 1925. Until recently very little interest has been shown in the friction disk principle. Since 1958 several groups have investigated the principle with varying degrees of success. Here again most of the testing has been directed toward the operation of the turbine rather than the pump. A summary of the results of several investigations is given in the next section.

Literature Survey

Rice [7] presents a summary of test results from a water pump and an air blower using multiple disk rotors. He also gives a first approximation mathematical analysis of the performance of such machinery. No attempt is made in the discussion to compare the experimental results with the analysis.

The water pump which was tested contained 34 disks, 5.0 inches in diameter. They were .020 inches thick and spaced .020 inches apart. The inlet was 1.0 inches in diameter and contained no shaft or other obstructions. The disks were supported by eight small throughbolts and an inlet spider at each side. Water entered from chambers in the pump housing, through the inlet spiders, into the central hollow portion of the rotor and finally into the spaces between the disks.

The efficiency was defined as the ratio of the increase in the hydraulic energy of the fluid through the pump to the shaft work supplied to the pump. The maximum efficiency reported for this unit was in the order of 20 percent.

The mathematical analysis was carried out by applying certain idealizations and assumptions to the Navier-Stokes equations. The

final results of the analysis agree closely with the linearized solution shown in the present paper. However, one important design parameter did not show up in the analysis. This parameter relates the disk spacing, the fluid kinematic viscosity and the angular velocity. In the present paper this parameter is found to be the key to determining the optimum design.

The investigation by Beans [1] was very similar to that of Rice. The mathematical approach was different but the results were similar. The lack of the design parameter discussed above limited the usefulness of the results.

The study by Hasinger and Kehrt [6] employed the results of the work by Breiter and Pohlhausen [2]. Their test apparatus was a water pump with the disks built in the shape of cones rather than flat as in most cases. This design produced a more rigid disk and reduced the inlet angle through which the fluid had to turn from the axial to the radial direction. The reported efficiency was near 60 percent and was defined as the total head gain divided by the sum of ideal pump head and the rotor-housing friction loss.

CHAPTER II

MATHEMATICAL ANALYSIS

This analysis is based on the results of a report by Pohlhausen and Breiter [2]. Their report investigates the viscous flow between two parallel disks which rotate with the same constant angular velocity in the same direction. The analysis determines the velocity distribution between the disks, the pressures, the torque applied at the shaft, and the resulting efficiency.

The problem was approached by applying the boundary layer assumptions to the equations of fluid motion (Navier-Stokes equations). Practical considerations justify this approach. The distance between the disks must be very small in order for viscous forces to produce a significant tangential flow. This assumption allowed the Navier-Stokes equations to be reduced to a system of parabolic differential equations.

The problem is described by a system of cylindrical co-ordinates as shown in Fig. 3. The Navier-Stokes and continuity equations which describe the imcompressible, axi-symmetric, steady, viscous flow are as follows:

$$u\frac{\partial V}{\partial r} + w\frac{\partial V}{\partial z} + \frac{uV}{r} = \nu\frac{\partial^2 V}{\partial z^2} + \nu\frac{\partial}{\partial r}\left(\frac{V}{r}\right) + \nu\frac{\partial^2 V}{\partial r^2}$$

$$u\frac{\partial W}{\partial r} + w\frac{\partial W}{\partial z} = -\frac{1}{\rho}\frac{\partial P}{\partial z} + \nu\frac{\partial^2 W}{\partial z^2} + \nu\frac{1}{r}\frac{\partial W}{\partial r} + \nu\frac{\partial^2 W}{\partial r^2}$$

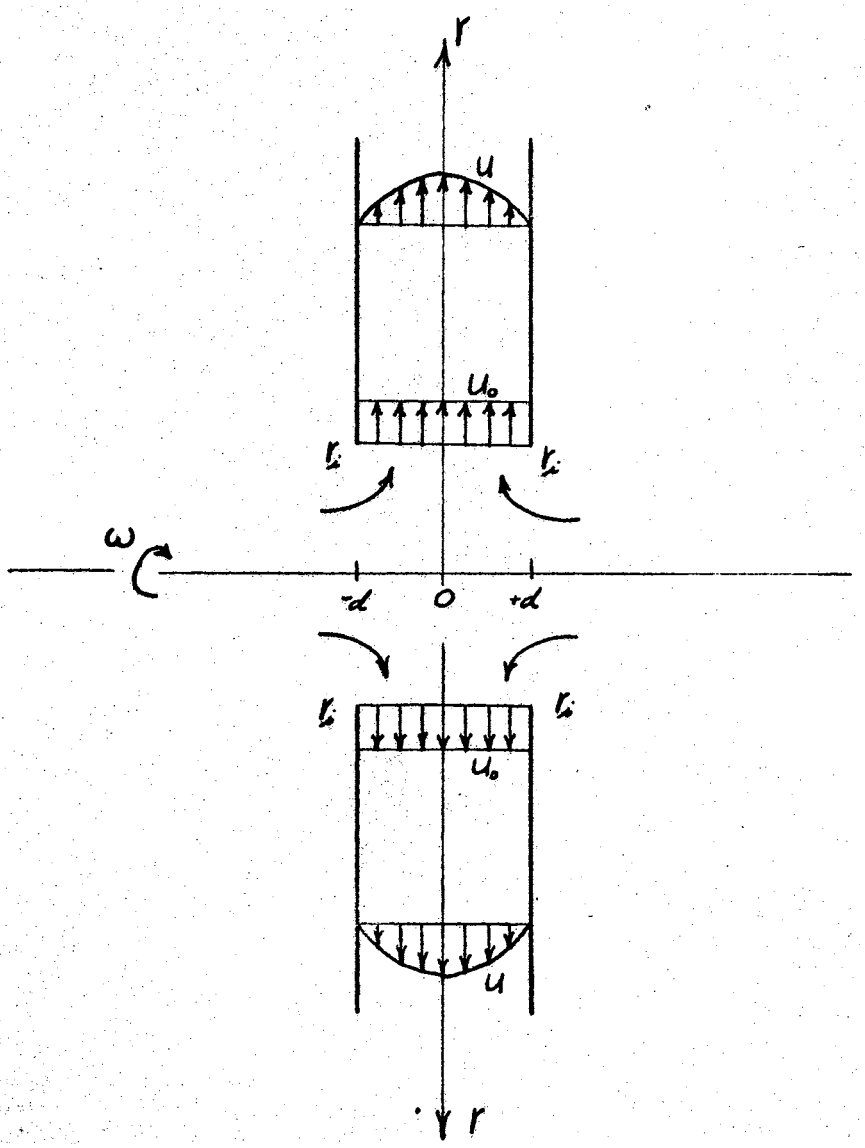

FIG. 3

SCHEMATIC DIAGRAM OF

THE FLOW BETWEEN TWO

ROTATING DISKS

$$u\frac{\partial u}{\partial r} + w\frac{\partial u}{\partial z} - \frac{v^2}{r} = -\frac{1}{\rho}\frac{\partial p}{\partial r} + \nu\frac{\partial^2 u}{\partial z^2} + \nu\frac{\partial}{\partial r}\left(\frac{u}{r}\right) + \nu\frac{\partial^2 u}{\partial r^2}$$

$$\frac{\partial u}{\partial r} + \frac{u}{r} + \frac{\partial w}{\partial z} = 0$$

Introduction of the boundary layer approximations results in the omission of the equation of motion in the axial direction. The system of equations is now reduced to

$$u\frac{\partial v}{\partial r} + w\frac{\partial v}{\partial z} + \frac{uv}{r} = \nu\frac{\partial^2 v}{\partial z^2}$$

$$u\frac{\partial u}{\partial r} + w\frac{\partial u}{\partial z} - \frac{v^2}{r} = -\frac{1}{\rho}\frac{\partial p}{\partial r} + \nu\frac{\partial^2 u}{\partial z^2}$$

$$\frac{\partial u}{\partial r} + \frac{u}{r} + \frac{\partial w}{\partial z} = 0$$

For convenience the tangential velocity v of the fixed co-ordinate system is now transformed to the tangential velocity V relative to the disks

$$V = v - r\omega$$

With this single transformation all velocities are now considered to be relative to the disks.

Introducing this transformation into the above expressions yields:

$$u\left[\frac{\partial V}{\partial r}+\omega\right]+w\frac{\partial V}{\partial z}+\frac{u[V+r\omega]}{r}=\nu\frac{\partial^2 V}{\partial z^2} \tag{2.1}$$

$$u\frac{\partial u}{\partial r}+w\frac{\partial u}{\partial z}-\frac{V^2+2Vr\omega+r^2\omega^2}{r}=-\frac{1}{\rho}\frac{\partial P}{\partial r}+\nu\frac{\partial^2 u}{\partial z^2} \tag{2.2}$$

$$\frac{\partial u}{\partial r}+\frac{u}{r}+\frac{\partial w}{\partial z}=0 \tag{2.3}$$

The boundary conditions along the disks are given by

$$u(r,\pm d)=0$$

$$v(r,\pm d)=0$$

$$w(r,\pm d)=0$$

And the velocity distribution at the entrance cross section is given by

$$u(r_i,z)=u_0$$

$$v(r_i,z)=-r\omega$$

$$w(r_i,z)=0$$

The solution of this non-linear system is now presented in two parts. The first part introduces assumptions which linearize the above equations and leads to a useful solution. These assumptions are not valid in the immediate neighborhood of the inlet region. Thus the second part is concerned with a numerical solution of the system near the inlet.

Linearized Solution

If it is assumed that the fluid velocities relative to the disks are small then quadratic terms involving these velocities can be

neglected. This condition is satisfied at all radii except near the inlet and results in a linear system which can be solved by standard techniques. The solution is considered to be an asymptotic expression for the actual system.

When the quadratic terms in U, V, and W are omitted from equations (2.1) and (2.2) the following expressions result:

$$U = \frac{\nu}{2\omega} \frac{\partial^2 V}{\partial z^2} \tag{2.4}$$

$$\frac{\nu}{\omega} \frac{\partial^2 U}{\partial z^2} + 2V = \frac{1}{\rho\omega} \frac{\partial P}{\partial r} - r\omega \tag{2.5}$$

The boundary layer assumption that the pressure does not depend upon Z allows equation (2.5) to be written in the form

$$\frac{\nu}{\omega} \frac{\partial^2 U}{\partial z^2} + 2V = F(r) \tag{2.6}$$

Equations (2.4) and (2.6) can be solved with the aid of the initial velocity and boundary conditions and the continuity equation (2.3).

It is found that the velocity profiles are governed by one dimensionless quantity which we will call the distance parameter. This parameter contains the angular velocity, the kinematic viscosity, and the distance between the disks. It is given by

$$\bar{d} = d\sqrt{\frac{\omega}{\nu}}$$

For the purpose of this investigation the most important results involve the determination of the pressure gradient. This is found to be

$$\frac{dP}{dr} = \rho\omega\left[r\omega - \frac{\sqrt{\frac{\omega}{\nu}}\, Q}{\pi r \beta}\right] \tag{2.7}$$

where

$$\beta = \frac{\sinh(2\bar{d}) - \sin(2\bar{d})}{\cosh(2\bar{d}) + \cos(2\bar{d})}$$

and Q is the volume flow rate which is given by

$$Q = 4\pi d r_i U_o \tag{2.8}$$

Equation (2.7) can be integrated to yield

$$P_e - P_i = \frac{\rho\omega^2}{2}(r_e^2 - r_i^2) - \rho\omega\sqrt{\frac{\omega}{\nu}}\,\frac{Q}{\pi\beta}\ln\left(\frac{r_e}{r_i}\right) \tag{2.9}$$

For simplicity the pressure, radius, and velocity terms can be non-dimensionalized:

$$\bar{P} = \frac{P}{\rho\omega^2 r_i^2} \qquad \bar{U}_o = \frac{U_o}{r_i\omega} \qquad \bar{r} = \frac{r_e}{r_i}$$

Inserting these into equations (2.8) and 2.9) yields

$$\bar{P}_s = \frac{1}{2}(\bar{r}^2 - 1) - \frac{Q}{\pi r_i^2\sqrt{\omega\nu}\,\beta}\ln\bar{r} \tag{2.10}$$

$$Q = 4\pi d\omega r_i^2 \bar{U}_o \tag{2.11}$$

where $\bar{P}_s$ is the dimensionless static pressure rise across the disks. Upon combining (2.10) and (2.11) and introducing the parameter $\bar{d}$, we find that the pressure can be expressed in terms of the radial inlet velocity by

$$\bar{P}_s = \frac{1}{2}(\bar{r}^2 - 1) - \frac{4\bar{d}\,\bar{U}_o}{\beta}\ln\bar{r} \tag{2.12}$$

This equation can be used to calculate the pressure rise for a given flow rate and rotor size. The maximum pressure will of course depend upon the value of the ratio $\frac{\bar{d}}{\beta}$. This ratio is shown in Fig. 4 as a function of $\bar{d}$. It is apparent that the maximum pressure will be obtained when the value of $\bar{d}$ is 1.1, the corresponding value of $\frac{\bar{d}}{\beta}$

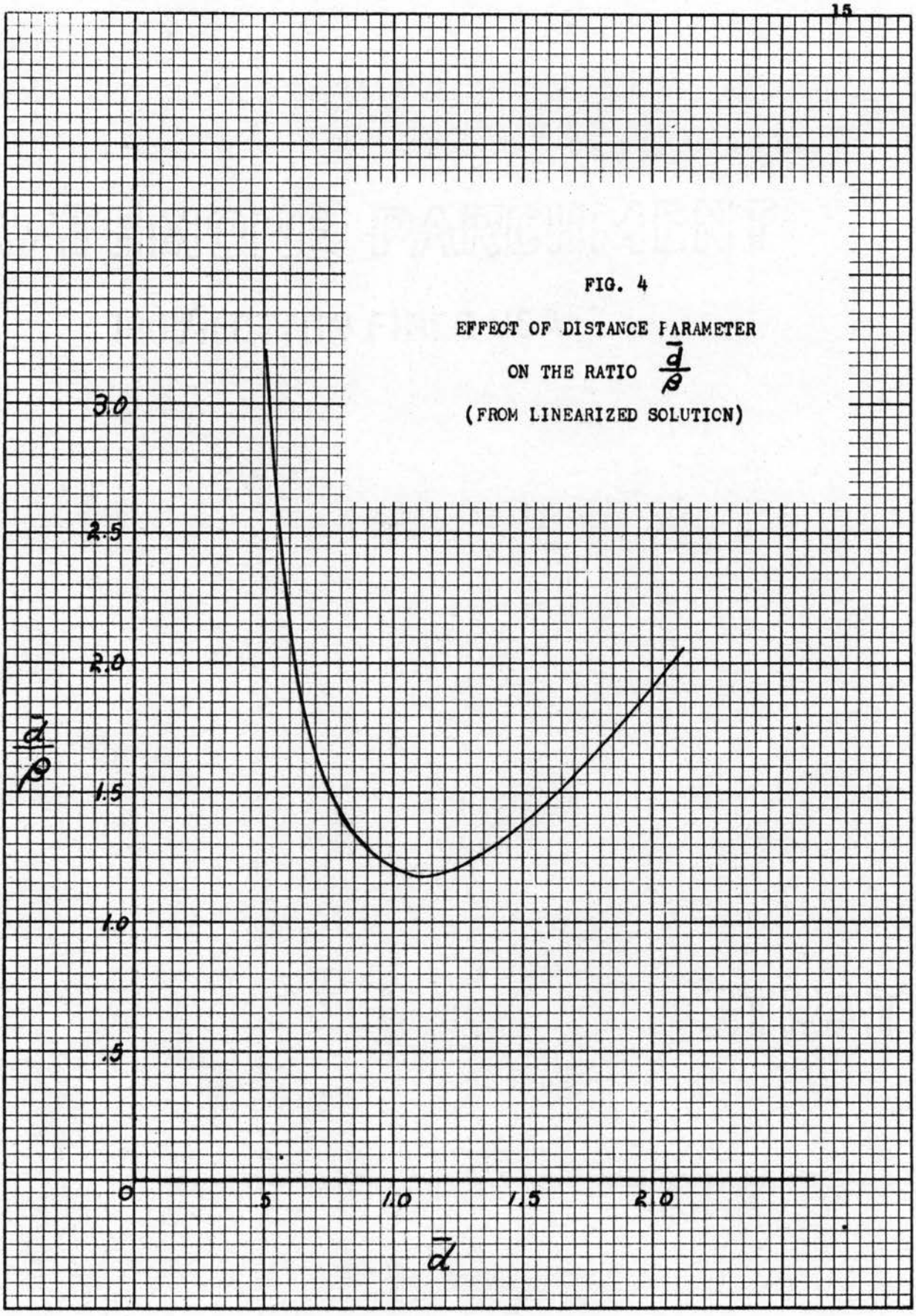

FIG. 4

EFFECT OF DISTANCE PARAMETER

ON THE RATIO $\frac{\bar{d}}{\rho}$

(FROM LINEARIZED SOLUTION)

is 1.17. This optimum value of the distance parameter is very important in the rotor design as it defines the relationship between the fluid viscosity, the disk spacing and the speed.

Numerical Solution

The simplifying assumptions of the previous solution led to a system of equations which were very useful from a design standpoint. However, as explained earlier these assumptions were not valid near the disk inlet. Since most of the losses occur in this region a solution to the non-linear system is important.

For the numerical integration of equations (2.1), (2.2), and (2.3) a new system of co-ordinates was introduced (Fig. 5) and a new set of dimensionless variables were used.

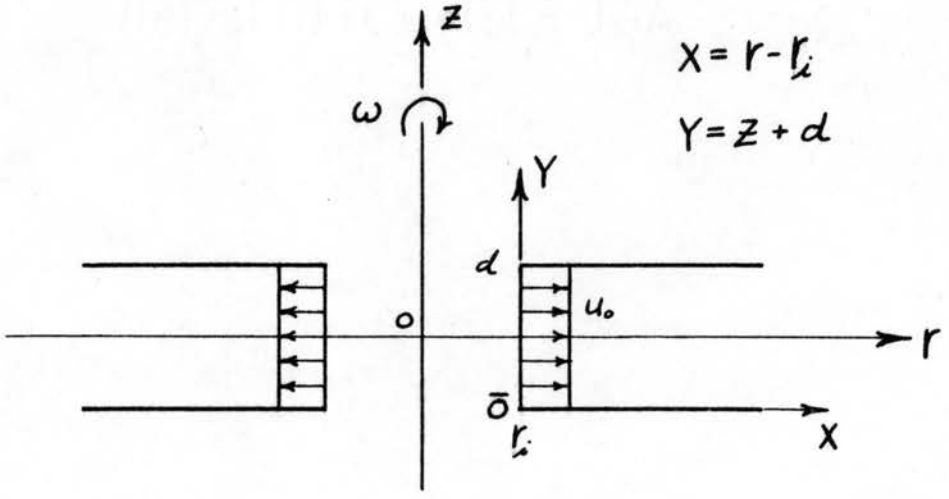

FIG. 5

TRANSFORMED CO-ORDINATE SYSTEM

USED IN THE NUMERICAL

SOLUTION

$$\bar{u} = \frac{u}{r_i \omega} \qquad \bar{x} = \frac{x}{r_i} \qquad \bar{r} = 1 + \bar{x}$$

$$\bar{v} = \frac{v}{r_i \omega} \qquad \bar{y} = y\sqrt{\frac{\omega}{\nu}} \qquad \bar{d} = d\sqrt{\frac{\omega}{\nu}}$$

$$\bar{w} = \frac{w}{\sqrt{\nu\omega}}$$

Introducing these new variables into equations (2.1), (2.2), and (2.3) the following system is obtained:

$$\bar{u}\frac{\partial \bar{u}}{\partial \bar{x}} + \bar{w}\frac{\partial \bar{u}}{\partial \bar{y}} - \bar{v}\left[\frac{\bar{v}}{1+\bar{x}} + 2\right] = -\bar{F}(\bar{r}) + \frac{\partial^2 \bar{u}}{\partial \bar{y}^2}$$

$$\bar{u}\left[\frac{\partial \bar{v}}{\partial \bar{x}} + \frac{\bar{v}}{1+\bar{x}} + 2\right] + \bar{w}\frac{\partial \bar{v}}{\partial \bar{y}} = \frac{\partial^2 \bar{v}}{\partial \bar{y}^2}$$

$$\frac{\partial \bar{u}}{\partial \bar{x}} + \frac{\bar{u}}{1+\bar{x}} + \frac{\partial \bar{w}}{\partial \bar{y}} = 0$$

where

$$\bar{F}(\bar{r}) = \bar{r} - \frac{1}{\rho \omega^2 r_i^2}\frac{dp}{dr}$$

The boundary conditions now become

$$\bar{u}(\bar{x}, 0) = 0 \qquad \frac{\partial \bar{u}(\bar{x}, \bar{d})}{\partial \bar{y}} = 0$$

$$\bar{v}(\bar{x}, 0) = 0 \qquad \frac{\partial \bar{v}(\bar{x}, \bar{d})}{\partial \bar{y}} = 0$$

$$\bar{w}(\bar{x}, 0) = 0$$

This system of equations was solved by Breiter and Pohlhausen using a modified 'inverse' difference procedure, and the results were shown in graphical form. Fig. 6 shows the dimensionless pressure versus radial inlet velocity for $\bar{d}=1.0$ with $\bar{r}$ as a parameter. The solid lines are from equation (2.12) and the dashed lines represent the non-linearized solution. The solution of the non-linearized problem was shown by Breiter and Pohlhausen in a plot of pressure

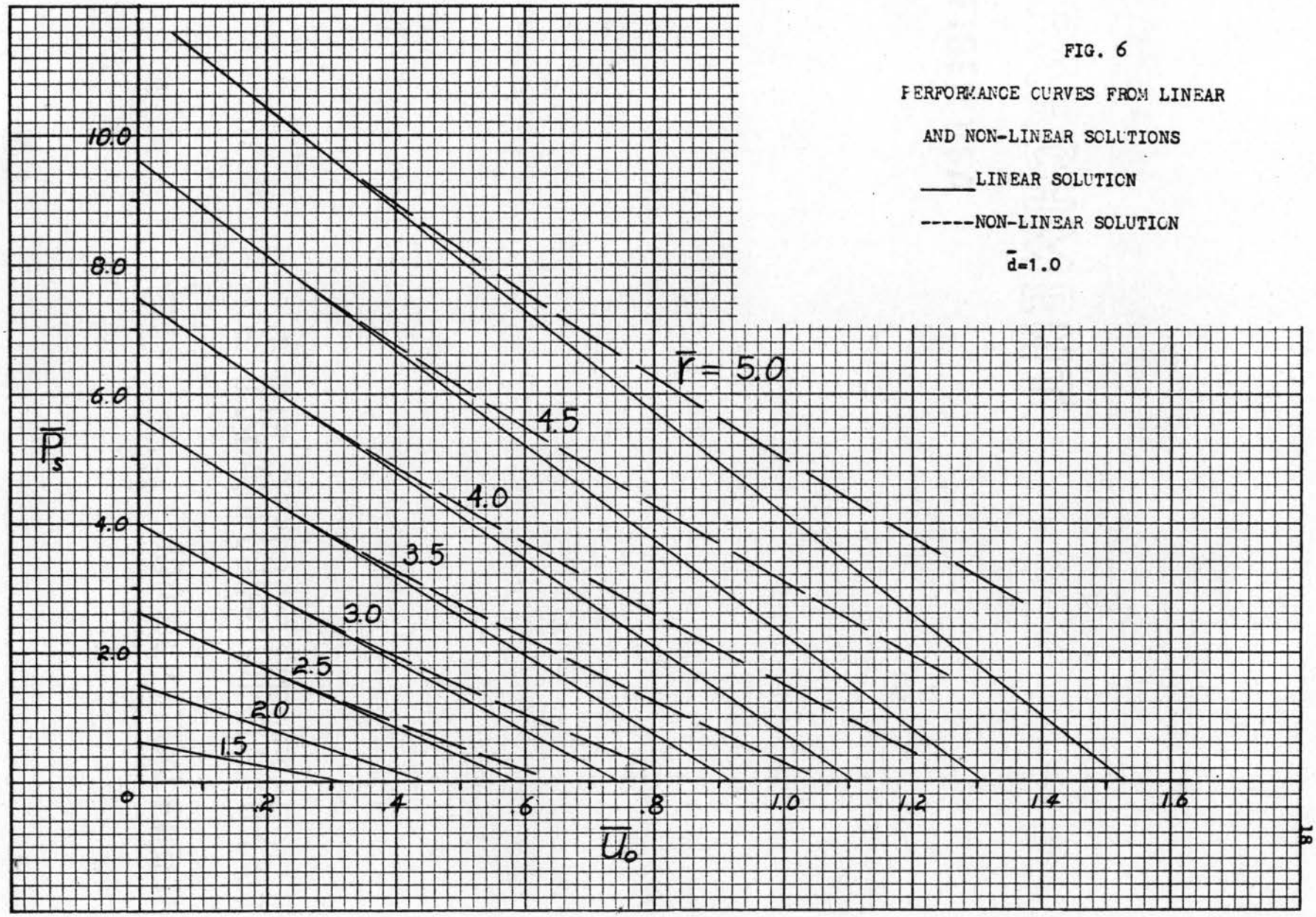

FIG. 6

PERFORMANCE CURVES FROM LINEAR AND NON-LINEAR SOLUTIONS

____ LINEAR SOLUTION

----- NON-LINEAR SOLUTION

$\bar{d}$=1.0

gradient versus $\bar{r}$ with $\bar{U}_o$ as a parameter and $\bar{d}$=1.0. Graphical integration was therefore necessary to produce the dashed curves of Fig. 6.

The rotor efficiency is defined by

$$\eta_R = \frac{P_s + P_d}{M\omega} Q$$

Fig. 7 shows the rotor efficiency as a function of $\bar{U}_o$ with $\bar{r}$ as a parameter.

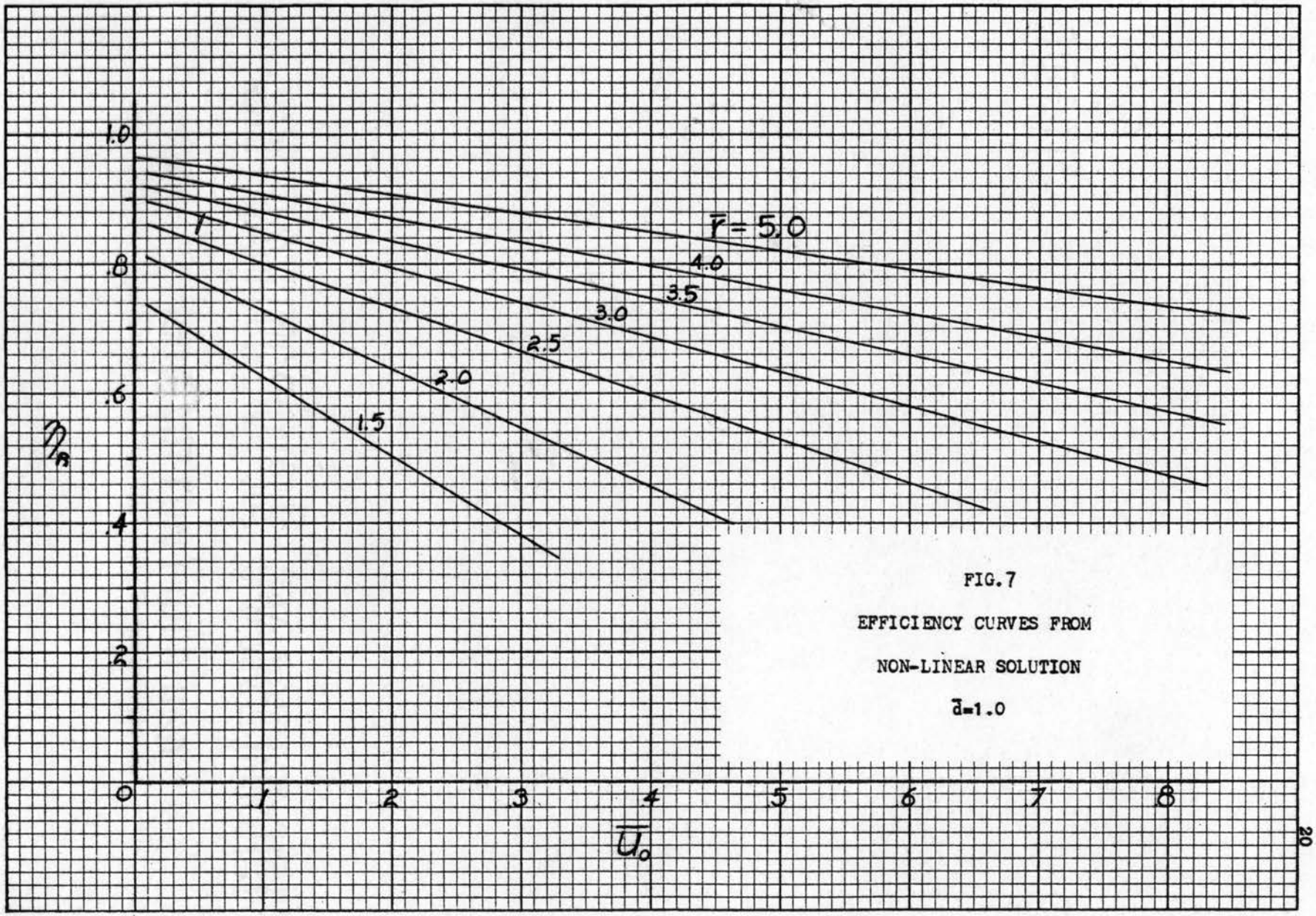

FIG. 7

EFFICIENCY CURVES FROM

NON-LINEAR SOLUTION

$\bar{d}$=1.0

CHAPTER III

TEST FAN DESIGN AND INSTRUMENTATION

A friction disk fan was built and tested in order to check the design parameters and performance which was predicted by the analysis in the previous chapter.

The fan consisted of a set of disks mounted on a shaft and surrounded by a plastic housing (Figs. 8-10). The function of the housing was to provide a means of controlling the outlet pressure. The efficient diffusion of the fluid stream was not an important factor in the design of the test fan because only the rotor section was being studied.

The housing was designed with the air inlet on one side and the driving motor on the other side. A more practical design would admit air from both sides but the single inlet arrangement was desired for test purposes. This was done so that the flow restriction in the inlet ports could be studied, as will be discussed later.

The most critical points in the fan design were the disks themselves and the seal between the housing and the first disk. To obtain satisfactory disks a material had to be selected which was of uniform thickness and stiff enough to remain absolutely flat after the machining operations. The requirement that the disk be flat and parallel is demonstrated by the dependence of $\bar{d}$ on the distance between adjacent disks.

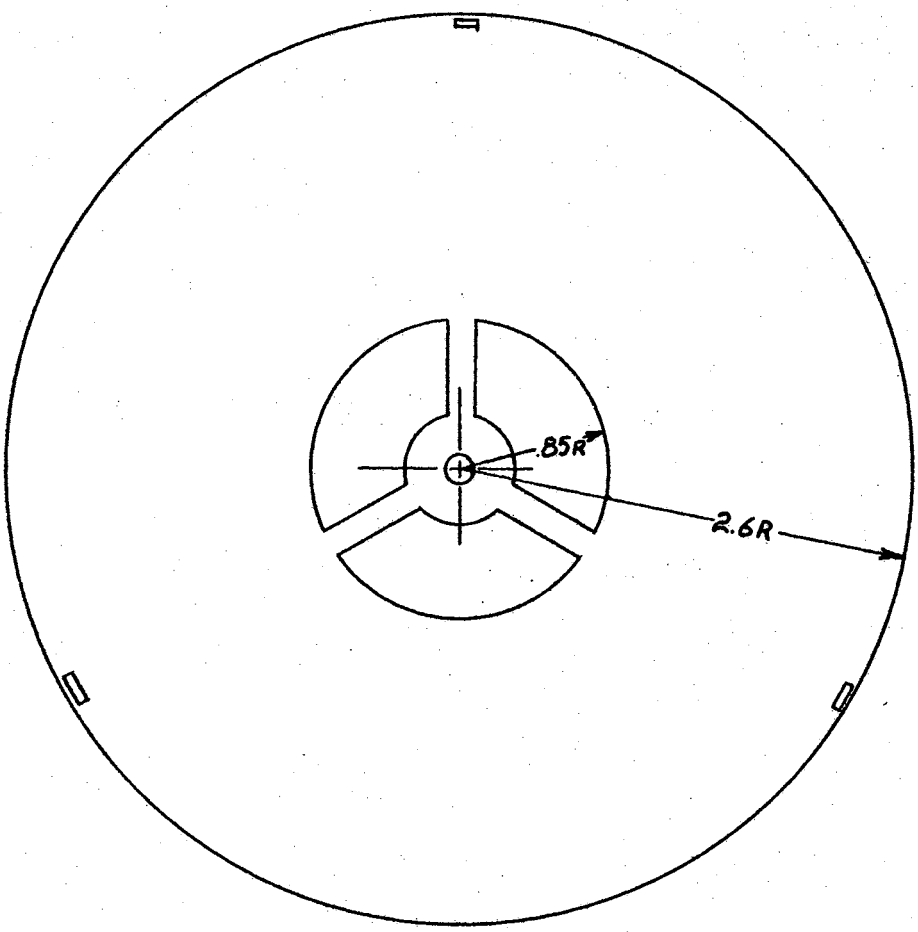

FIG. 8

DETAILS OF DISK DESIGN

$\bar{r}$=3.06

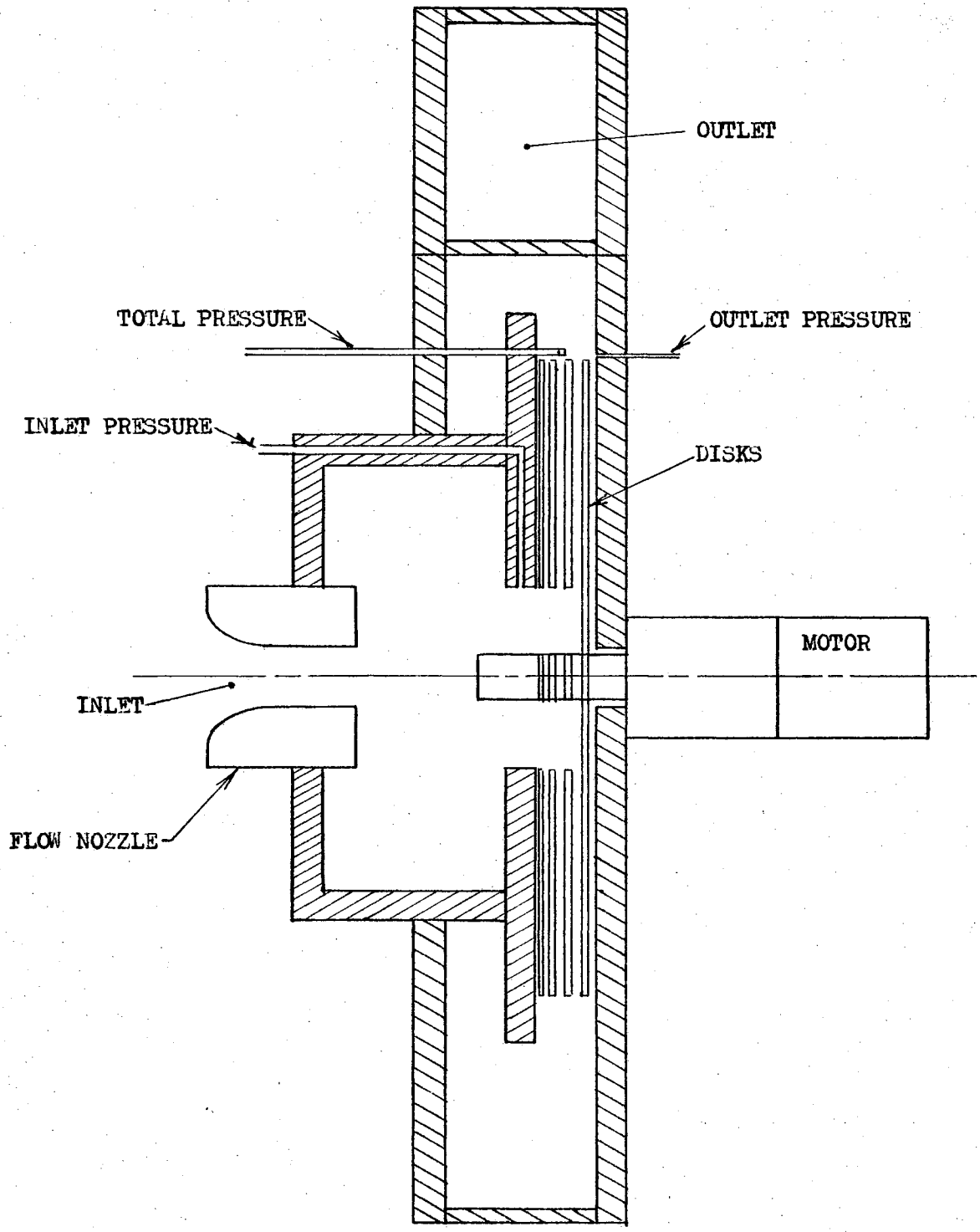

FIG. 9

TEST FAN SIDE VIEW

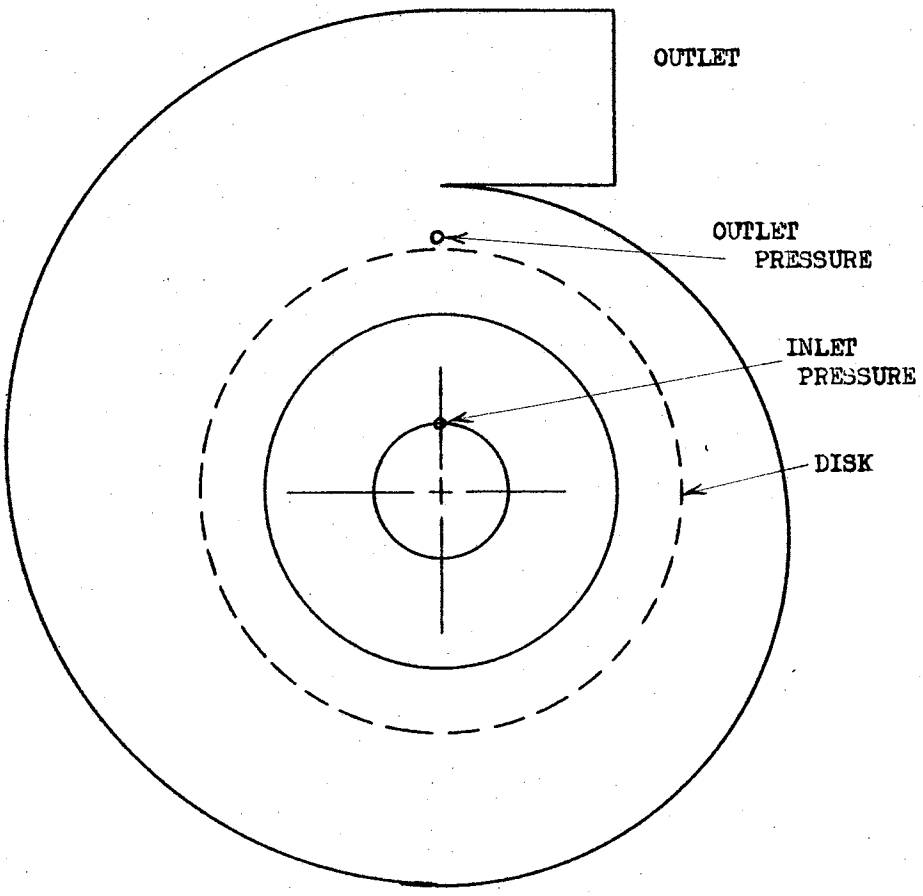

FIG. 10

TEST FAN FRONT VIEW

The disks used in the tests were made of 0.056 inch acrylic plastic. This material was of uniform thickness but was not as flat as desired. The disks had to be held parallel by placing small spacers at the outer radius. In order to reduce the pressure loss at the seal between the housing walls and the adjacent disk, a solid disk was used at the motor end of the fan and a special wall was built which could be positioned very carefully at the inlet side.

Two sets of disks were used in the test fan. The outside diameters were held constant at 5.2 inches and the inside diameters were 1.7 inches and 2.6 inches resulting in radius ratios of 3.06 and 2.0 respectively. The total area of the inlet ports was reduced in each case by the presence of the shaft and the disk spokes. The disk spacing remained constant at 0.025 inches throughout the testing program. The value of $\bar{d}$ was controlled by the speed of the driving motor.

Internal stresses in the material caused by the high rotational speeds were never a significant problem and were calculated by treating the disks as spoked flywheels.

The flow rate was measured at the fan inlet with an A.S.M.E. flow nozzle.

To calculate the rotor efficiency it was desired only to measure the power necessary to pump the air through the rotor[2]. Thus the power requirement would be zero when the flow rate was zero. The fan was

---

[2]All losses external to the rotor, e.g. motor efficiency, housing to rotor friction losses, were not included in this efficiency.

driven by a 6 volt D.C. motor which was controlled by a variable voltage power supply. The power input was measured by the current and voltage supplied to the motor. Bearing friction and viscous losses between the solid wall and the first moving disk were carefully held constant during each test. Therefore they would cancel out in the calculations. A typical power requirement curve is shown in Appendix A, Fig. 17. In this figure the above mentioned losses control the position (height) of the curve and the power required by the rotor determines the slope of the curve. Thus to calculate the rotor efficiency only the slope of the curve is necessary.

The mathematical analysis required that the pressure measurements be made at points between the disks at the inner and outer radii. This requirement was quite difficult to satisfy because of the rotation of the disks and the size of the gap between them. It was therefore necessary to make all pressure measurements outside of the disks (Fig. 9).

The inlet static pressure was measured at a point in the wall of the inlet port. The pressure here can be corrected to the actual inlet pressure by considering two factors[3]. First, the difference in the flow area between the inlet and the disk gap will cause a velocity change which will influence the pressure. The influence of this area difference was calculated and found to be small, so it was neglected. The second factor concerns the tangential velocity increase due to the rotation of the disk spokes. It was not possible to measure the extent of the velocity increase due to this factor in the test fan.

---

[3]These calculations are shown in Appendix B.

The calculations show that a significant correction would be necessary if the air velocity approached the velocity of the disks before it entered the gap.

The outlet static pressure was measured at a point in the housing wall and as close to the edge of the disks as possible. The outlet dynamic pressure was measured with a total head probe. This probe could be positioned directly over the disk gap and rotated to determine the maximum pressure. The dynamic pressure measured by this probe was an average value because the opening in the probe was the same size as the disk gap.

A correction factor at this point would be determined by the amount of diffusion which took place between the disk outlet and the measuring points. The diffusion in this case was neglected because of the high exit velocity and the short distance between the disks and the measuring instruments, (Figs. 9 and 10).

CHAPTER IV

EXPERIMENTAL RESULTS

The material presented in the mathematical analysis indicated that the friction disk rotor is capable of achieving high values of efficiency. The real test of the friction disk principle is whether this efficiency can be realized in a practical design.

Fig. 11 shows the efficiency of the test rotor as a function of $\bar{U}_o$. This can be compared to Fig. 7 from the analysis. The performance curves are shown in Figs. 12 and 13 for both the experimental and analytic results. From this information it can be seen that the fan does have a reasonable efficiency but there is still a considerable amount of improvement which can be made.

There are two factors which should be considered when accounting for the losses indicated in these figures. These factors are pressure losses due to obstructions in the flow pattern, and uneven axial distribution of the flow.

Before looking into these points it would be well to review the assumptions which were made in the mathematical analysis. The mathematical model consisted of two flat parallel disks with a circular inlet at their center. The fluid was assumed to enter the region between the disks with zero tangential velocity and a uniform radial velocity U_o. The pressure rise was taken as the difference of the static pressures at the outer radius and the inner radius. All three

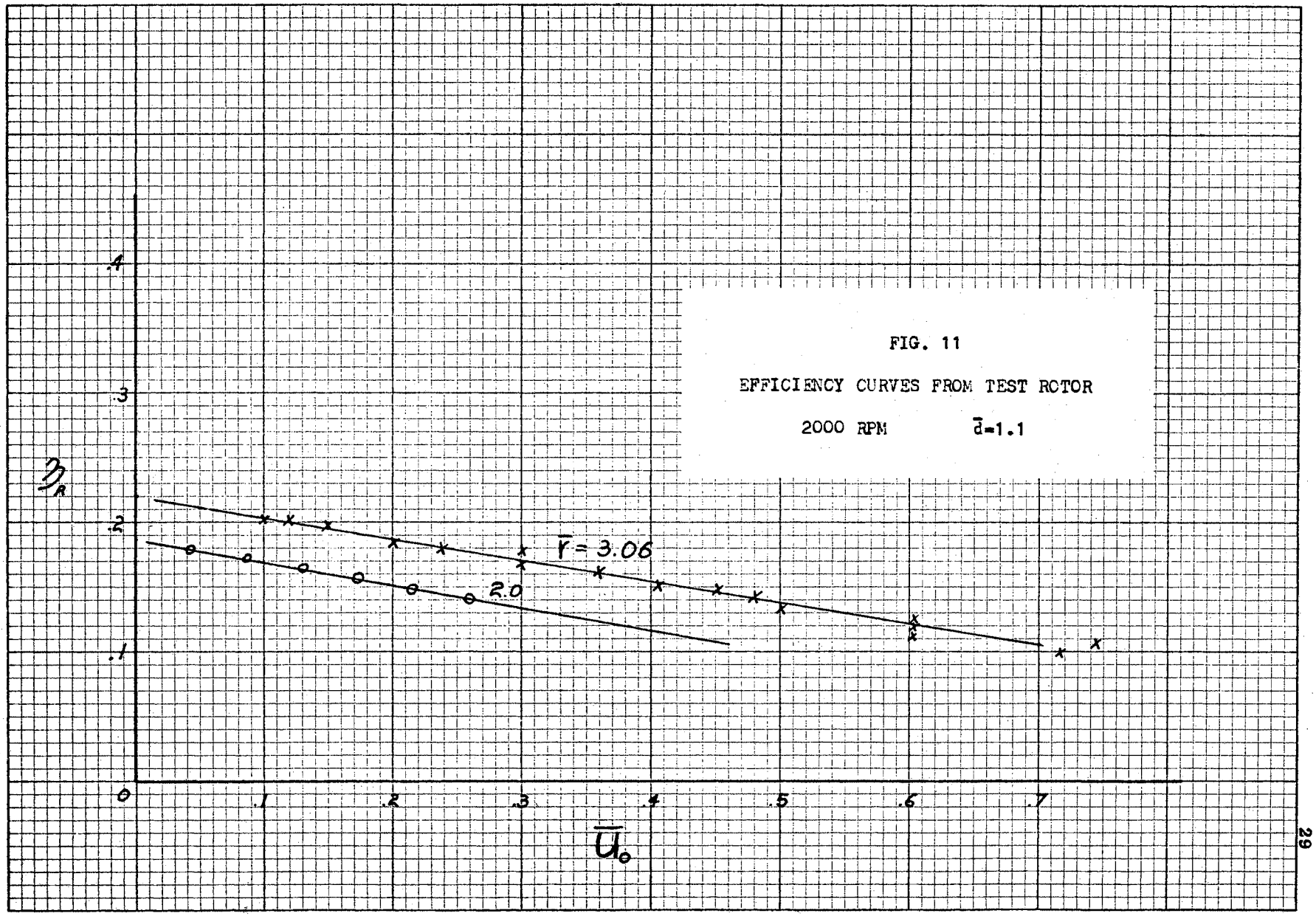

FIG. 11

EFFICIENCY CURVES FROM TEST ROTOR

2000 RPM $\bar{d}$=1.1

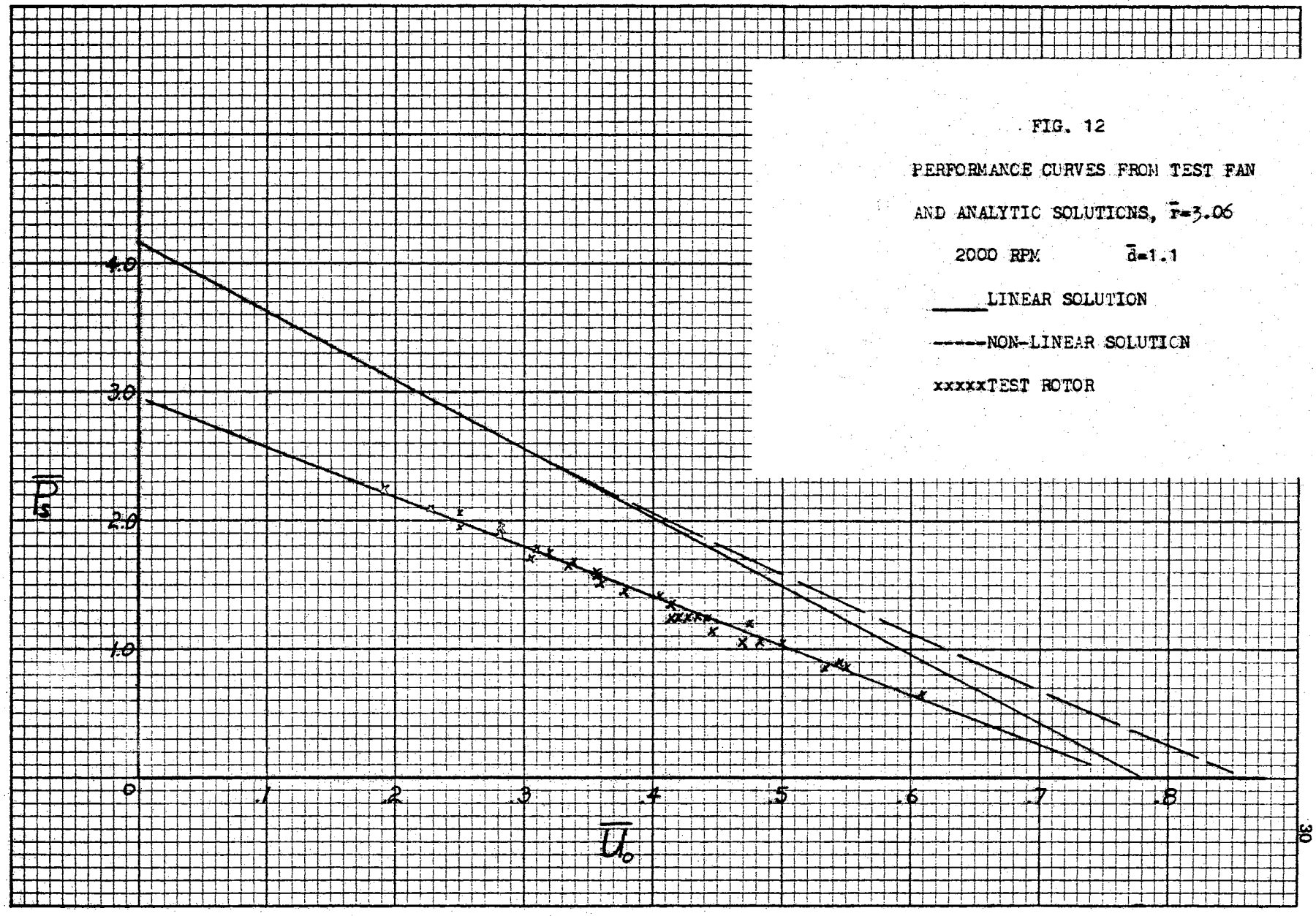

FIG. 12

PERFORMANCE CURVES FROM TEST FAN AND ANALYTIC SOLUTIONS, $\bar{r}=3.06$

2000 RPM $\bar{d}=1.1$

____ LINEAR SOLUTION

_ _ _ _ _ NON-LINEAR SOLUTION

xxxxx TEST ROTOR

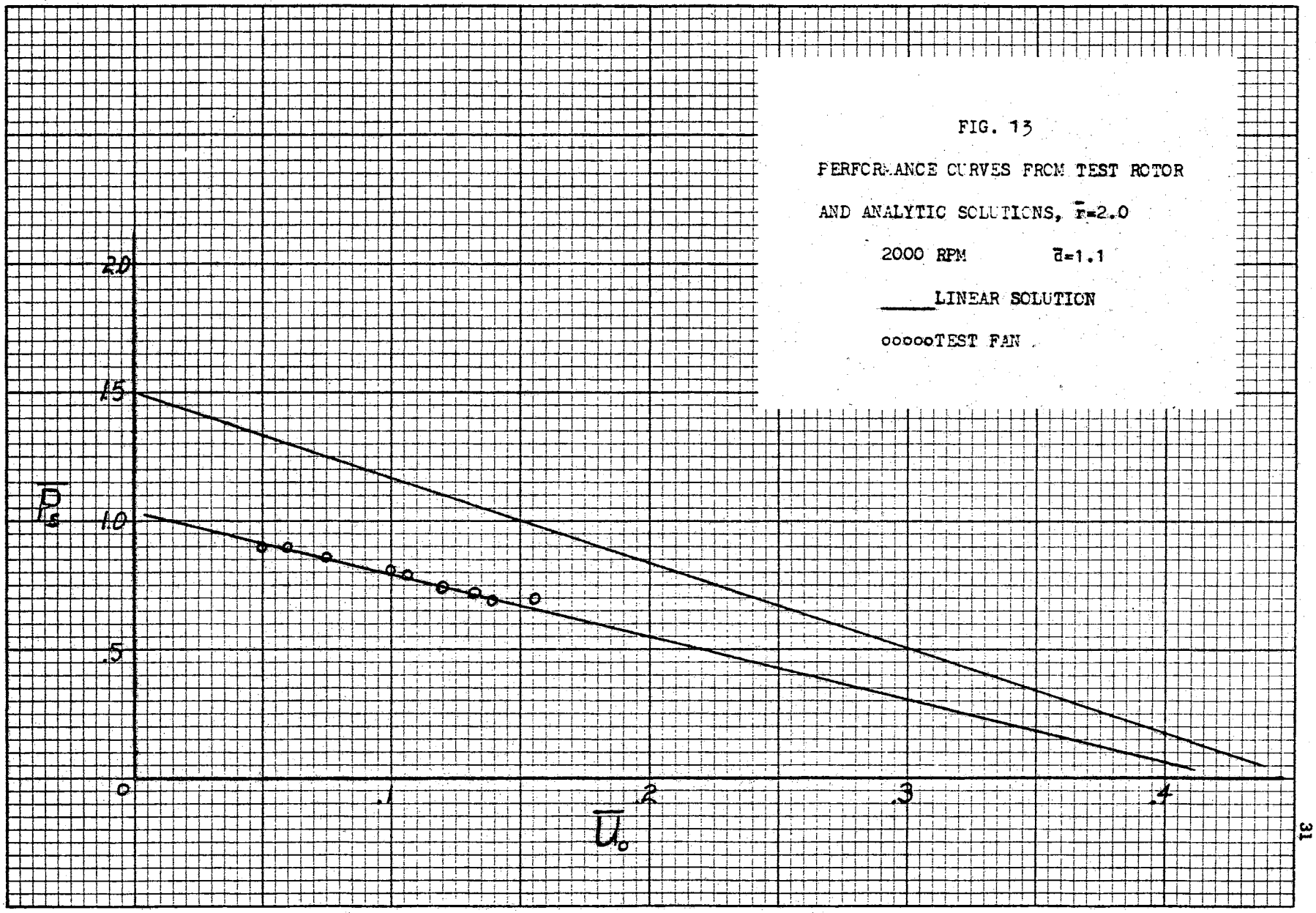
FIG. 13
PERFORMANCE CURVES FROM TEST ROTOR
AND ANALYTIC SOLUTIONS, $\bar{r}$=2.0
2000 RPM $\bar{d}$=1.1
LINEAR SOLUTION
oooooTEST FAN
20
15
1.0
.5
0
$\bar{P}_s$
.1
.2
.3
.4
$\bar{U}_o$

of these conditions were violated to some extent in the test model.

1) Pressure Losses - The disks in the test model were designed to fit those of the mathematical model as closely as possible but there were several difficulties which could not be overcome. One of these was the presence of the supporting shaft and the spokes which held the disks. The spokes acted as obstructions moving perpendicular to the flow which imparted a tangential velocity to the fluid. The obstruction also created a turbulent region which reduced the total pressure in the inlet. A second pressure loss occured in a turbulent region at the outer disk radius. This was caused by the presence of the small spacers between the disks.

2) Axial Flow Distribution - If the fan is to pass the flow rate for which it is designed, the fraction of the total flow which passes between each pair of disks must be the same. The flow rate for each disk pair can be measured by the dynamic pressure head at the outer radius. The maximum pressure measured in this manner will consist of two components, tangential and radial, both of which are functions of the flow rate. Thus the dynamic pressure produced by each disk pair will be an indication of the magnitude of the flow passing through them.

Fig. 14 shows the dynamic pressure developed by each pair of disks for a fan containing six disks with a radius ratio of 3.06. It is quite obvious that the flow is concentrated between the third and fourth disks (identical curves) and that the other disks are contributing very little to the total flow rate. A similar test was conducted with a radius ratio of 2.0. The results were identical except that the slope of curve No. 2 was brought up to equal that of curves 3 and 4.

FIG. 14

AXIAL FLOW DISTRIBUTION

$\bar{r}$=3.06 n=6

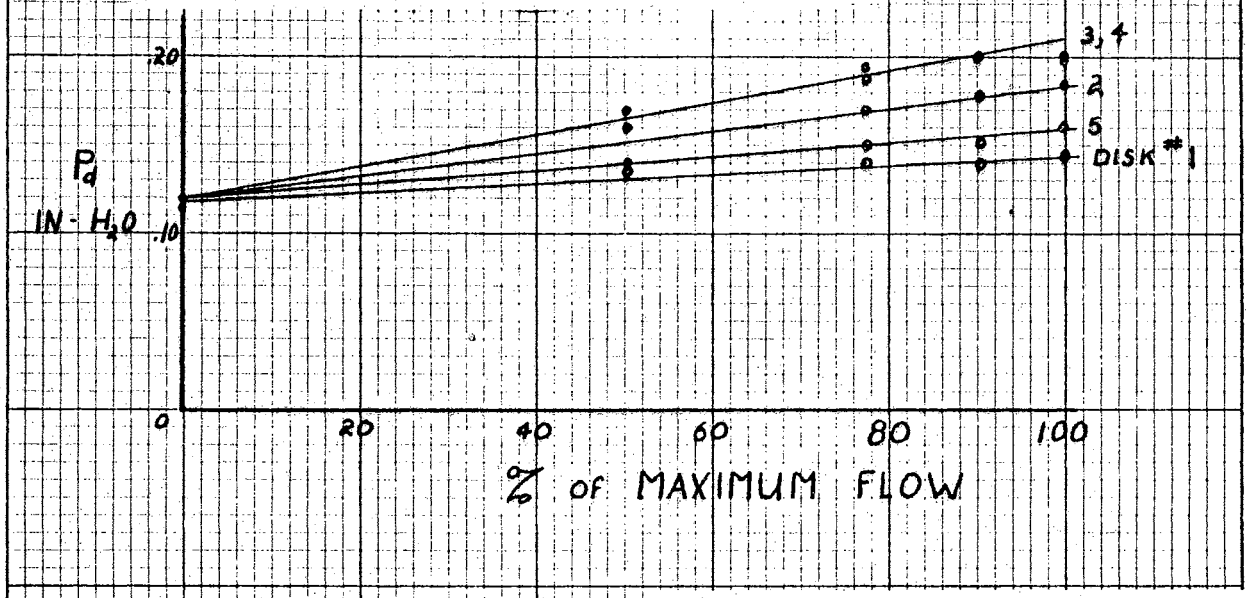

FIG. 15

EFFECT OF DISTANCE PARAMETER

ON TEST ROTOR EFFICIENCY

$\bar{r}$=2.0 n=6

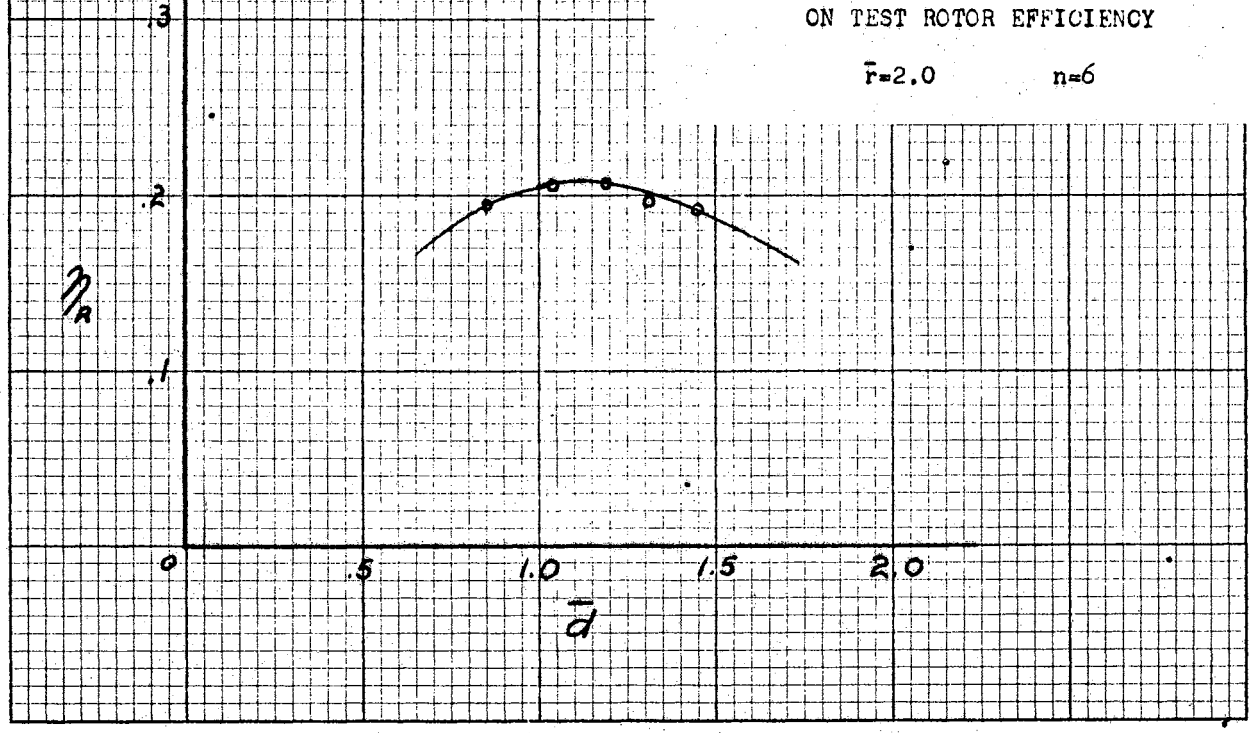

It was shown earlier that the maximum static pressure developed by the rotor would depend on the value of the distance parameter $\bar{d}$. Since the static pressure is related directly to the rotor efficiency it can be seen that selection of the proper value of $\bar{d}$ is very important in the design of the rotor. Fig. 15 shows the results of a test which was made to determine the optimum value of this parameter. It can be seen that the efficiency is maximum when $\bar{d}=1.1$ which serves to verify the results of the mathematical analysis.

As yet there has been no mention of the power required to drive the fan. The mathematical analysis did not cover this point except to show a graph of torque versus $\bar{r}$ with $\bar{U}_o$ as a parameter. This graph was a result of the numerical solution so that an equation was not given. It was therefore necessary to derive an empirical equation for the power requirement.

A series of tests were run to determine the relationship between power and flow rate with speed and radius ratio parameters. From this data it was found that the power was related directly to the mass flow and to the square of the speed. Also the power appeared to be independent of the radius ratio. Therefore, it was assumed to be a function of the outside radius only, as this had been held constant during the tests.

This information yields the following function:

$$HP = f(\rho Q \omega^2 r_e^n)$$

In order to make this function dimensionally correct the exponent n must be equal to 2 so that

$$HP \propto \rho Q \omega^2 r_e^2 \bar{r}^2$$

This equation was then compared to the graph shown by Breiter and Pohlhausen [2] and found to be very nearly correct with a constant of proportionality of 1.0. The modified equation is

$$HP = Q \rho \omega^2 r_t^2 (\bar{r}^2 - 1) \qquad (4.1)$$

The equation for the rotor efficiency given in the analysis can now be put into a simplified form. By non-dimensionalizing the pressure term and substituting equation (4.1) we find that

$$\eta_R = \frac{\bar{P}_s + \bar{P}_d}{(\bar{r}^2 - 1)} \qquad (4.2)$$

It appears that this equation may be very useful for determining the rotor efficiency in a practical case. A word of caution is therefore necessary. Any loss or deviation from ideal performance which occurs in the rotor will result in an actual power requirement which is higher than that predicted by equation (4.1). The result will be an actual efficiency which is lower than that given by equation (4.2)

CHAPTER V

APPLICATION OF DESIGN INFORMATION

The purpose of this investigation, as outlined in the introduction, was to obtain practical design information on a friction disk rotor. In this chapter the results will be put into a useful form and a practical method of design outlined.

General Design Method

The experimental results have shown that the expressions which were given in the analysis can be used to approximate the actual performance provided certain correction factors are used. These correction factors should be applied to the design pressure and to the number of disks to be used.

The design pressure can be corrected by adding a small amount to the dimensionless design pressure $\bar{P}$. This amount will usually be about 0.5 and can be approximated from the difference between the ideal and experimental curves in Figs. 12 and 13. It should be noted that the equation being used is from the linear solution and therefore is not exact. For this reason the pressure correction may become negative at high values of $\bar{U}_o$ and $\bar{r}$.

A second correction factor should be included to account for the flow distribution. This would be in the form of an increase in the number of disks to be used over the calculated number. The earlier

discussion of flow distribution indicates that the addition of one disk at each end would be sufficient for this correction.

In any design situation there are several variables which will be specified and others which will be determined by the operating conditions. The variables which are specified are usually the system resistance or pressure, the flow rate, the air density and the kinematic viscosity. The power source is usually known in advance so that the rotor speed can be determined. From these conditions the disk spacing can be found by using the distance parameter $\bar{d}$. The quantities which remain to be determined are the inside radius, the radius ratio, the number of disks, the dimensionless flow ratio $\bar{U}_o$ and the power requirement.

The inside radius will determine the inlet area and thus the velocity of the entering fluid. If the inlet area is too small the resulting high inlet velocity may produce an undesirable axial pressure drop. The maximum inlet velocity attained in the test fan was 6 ft/sec. and at this velocity there was no noticeable pressure loss. Thus the inside radius can be found from the required flow rate and the desired inlet velocity. The size of the shaft and the disk spokes must also be accounted for when calculating the inlet area. The required inlet radius can be reduced considerably by designing the fan to admit air from both ends. This is very desirable because the outside radius, thus the overall size of the unit, would be reduced by a similar amount.

The remaining variables can be determined from equations (2.11), (2.12), and (4.1).

Equation (2.11) expresses the flow rate for one pair of disks.

The total flow through the fan can be found by multiplying this flow rate by the number of pairs of disks. The final form of the flow equation is given by equation (2.11a)

$$Q = 4\pi d \omega r_i^2 \bar{U}_o (n-1) \qquad (2.11a)$$

$$\bar{P} = \frac{1}{2}(\bar{r}^2 - 1) - \frac{4\bar{d}\bar{U}_o}{\beta} \ln \bar{r} \qquad (2.12)$$

$$HP = Q \rho \omega^2 r_i^2 (\bar{r}^2 - 1) \qquad (4.1)$$

where

$$\bar{P} = \frac{P}{\rho \omega^2 r_i^2} \qquad \bar{r} = \frac{r_e}{r_i} \qquad \bar{d} = d\sqrt{\frac{\omega}{\nu}}$$

$$S = 2d$$

Equation (2.11a) should be solved first, keeping in mind that the efficiency will suffer as $\bar{U}_o$ is increased and that a large number of disks may present design problems. After the dimensionless pressure and flow ratios have been determined the radius ratio can be found from equation (2.12). To aid in the solution of this equation it is shown in Fig. 16 with $\bar{r}$ as a parameter. The power required to drive the fan can be calculated from the expression (4.1). Here again a correction factor must be employed. The power requirement of the test rotor was always about twice the amount given by this equation. In addition the power source must also be made large enough to overcome the resistance of the shaft bearings and the viscous resistance between the disks and the housing walls. An example problem will now be worked to illustrate the design method.

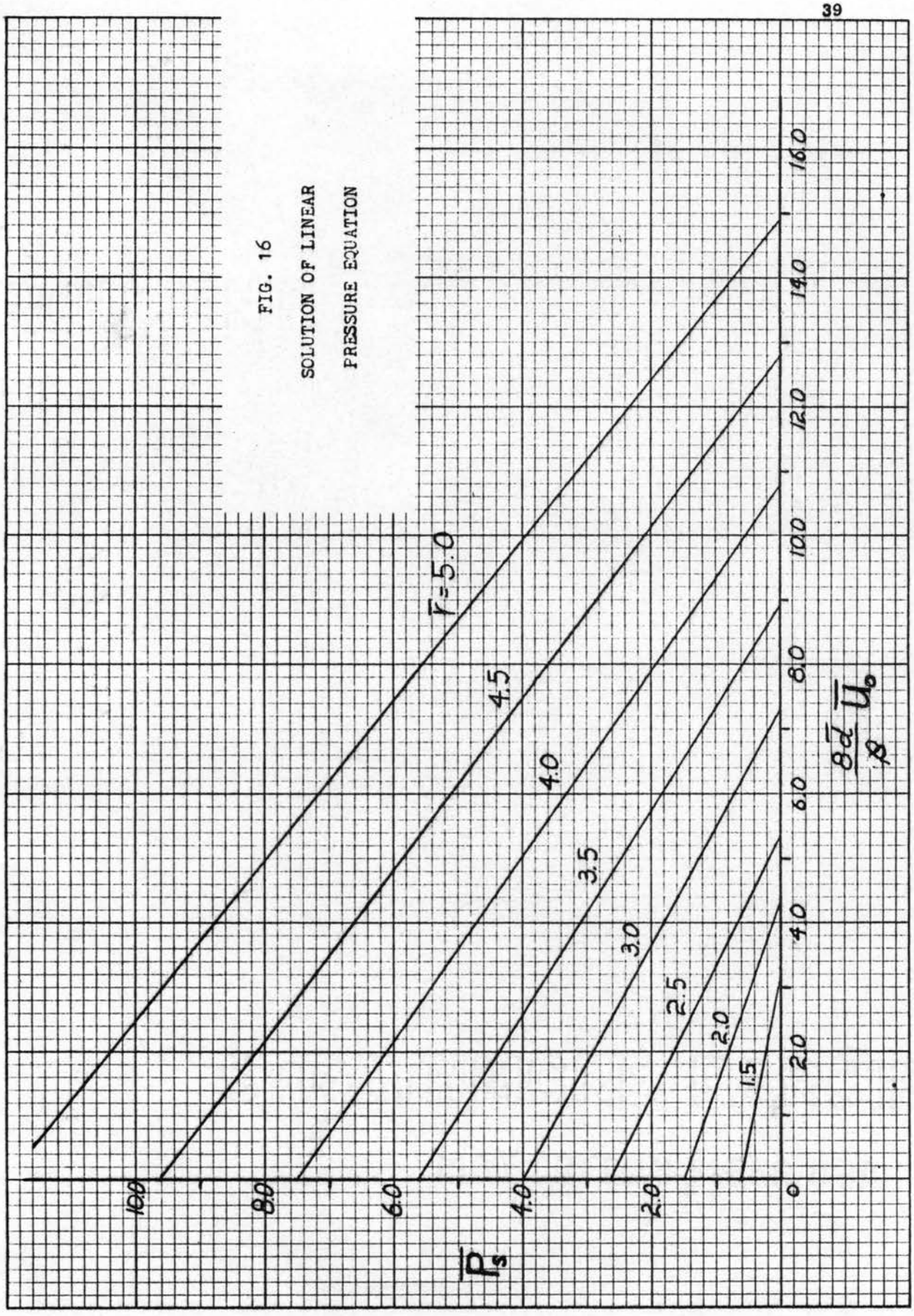

FIG. 16

SOLUTION OF LINEAR

PRESSURE EQUATION

Example Problem

Objective: Specify the critical dimensions of a friction disk rotor which will deliver 100 cfm of air at a static pressure of 0.5 inches H_2O. The rotor is to be driven by an electric motor which operates at 1150 RPM. Assume that the air density and kinematic viscosity are 2.24×10^{-3} Lbf sec^2/ft^4 and 1.7×10^{-4} ft^2/sec respectively and that flow will be admitted from both ends of the shaft.

Solution: First determine the angular velocity ω from the design speed:

$$\omega = RPM \frac{2\pi}{60} = 120.5$$

The disk spacing is determined from the optimum value of the distance parameter.

$$\bar{d} = d\sqrt{\frac{\omega}{\nu}}$$

$$d = \frac{1.1}{\sqrt{\frac{120.5}{1.7 \times 10^{-4}}}} = \frac{1.1}{840} = 1.31 \times 10^{-3} FT$$

$$d = .0157 \ IN$$

$$S = 2d = .0314$$

Since flow is admitted from both ends of the shaft the inside radius can be found from one half of the flow rate and the maximum inlet velocity. We will assume that a maximum inlet velocity of 10 ft/sec. is permissable without incurring a large axial pressure drop. Also we will reduce the area of the required inlet circle by 10% to allow for the area of the shaft and disk spokes.

$$\frac{Q}{2} = .9 AV$$

$$Q = 1.8\,\pi\, r_i^2\, V$$

$$r_i = \sqrt{\frac{Q}{1.8\pi V}} = \sqrt{\frac{100\ \frac{FT^3}{MIN}}{1.8\ \pi\ 10\ \frac{FT}{SEC}\ 60\ \frac{SEC}{MIN}}}$$

$$r_i = .172\ FT$$

$$r_i = 2.06\ IN$$

Equation (2.11a) can now be solved for the number of disks and the dimensionless radial velocity.

$$\bar{U}_o(n-1) = \frac{Q}{4\pi d \omega r_i^2} \qquad \frac{100\ \frac{FT^3}{MIN}\ \frac{MIN}{60\ SEC}\ \frac{1728\ IN^3}{FT^3}}{4\pi\ .0157\ IN\ \frac{120.5}{SEC}\ (2.06)^2\ IN^2}$$

$$\bar{U}_o(n-1) = 28.5$$

If we set $\bar{U}_o = 0.5$ then

$$n-1 = 57$$

To allow for axial flow distribution we will specify that 60 disks be used. The given supply pressure can be non-dimensionalized as follows:

$$\bar{P} = \frac{P}{\rho \omega^2 r_i^2} = \frac{0.5\ IN\ H_2O\ \left(.0361\ \frac{LB}{IN^2\ (IN\ H_2O)}\right)\ (144)^2\ \frac{IN^4}{FT^4}}{2.24 \times 10^{-3}\ \frac{LB\ SEC^2}{FT^4}\ \frac{(120.5)^2}{SEC^2}\ (2.06)^2\ IN^2}$$

$$\bar{P} = 2.72$$

Fig. 12 indicates that this value should be increased by about 0.6 to allow for inlet losses, thus $\bar{P} = 3.3$

The radius ratio can now be found with the aid of Fig. 16. Note that from Fig. 4 the optimum value of $\frac{\bar{\alpha}}{\beta}$ is 1.17, thus

$$8\,\frac{\bar{d}}{\beta}\,\bar{U}_o = 8\,(1.17)(.5) = 4.68$$

From Fig. 16 we find that $\bar{r} = 3.75$. The power requirement is given by equation (4.1).

$$HP = Q \rho \omega^2 r_i^2 (\bar{r}^2 - 1)$$

$$HP = \frac{100 \frac{FT^3}{MIN} \; 2.24 \times 10^{-3} \frac{LBF \; SEC^2}{FT^4} \; \frac{(120.5)^2}{SEC^2} (2.06)^2 IN^2 (3.75^2 - 1)}{144 \frac{IN^2}{FT^2} \qquad 33000}$$

$$HP = 0.0378$$

To account for losses in the disks this figure should be doubled, resulting in a power requirement of about 0.08 HP. If the bearing and housing friction losses are held to a minimum in the final design a 0.1 HP motor would be sufficient to drive the fan.

A summary of the final dimensions is as follows:

Disk Spacing	0.0314 Inches
Inside Radius	2.06 Inches
Number of Disks Required	60
Outside Radius of Disks	7.73 Inches
Motor Size	0.1 HP

This example is intended to serve as a guide in the use of the material presented in the paper. It should be remembered that only the rotor section has been considered here. The addition of a housing with a well designed diffuser section would increase the static pressure rise considerably.

CHAPTER VI

CONCLUSIONS

The analytical and experimental investigations have supplied information from which a friction disk rotor can be designed. The experimental results agreed reasonably well with the mathematical analysis and also indicated the magnitude of efficiency which can be expected from a practical design. There are several factors which limited the performance and efficiency of the test fan. The main limiting factors were the presence of the shaft and disk spokes in the inlet region, the spacers at the disk outlet and the lack of a positive seal between the housing and the disks. Most of these points could be eliminated or improved by redesigning the unit. Other investigations [5], [6] have indicated that the obstructions in the inlet region may have a considerable effect on the efficiency. The rotor designs in these references used throughbolts and spacers near the outer edge of the disks. In this manner the entire inlet circle was made available for the inlet port. Also the use of a cone shape increases the strength of the disks and reduces the angle through which the fluid must be turned before entering the disk gaps.

This type of fan has several inherent advantages over other types. There is no vibration problem caused by vanes passing by the diffuser outlet, and there are no lifting surfaces which can lead to flow separation. Both of these factors lead to undesirable noise

levels in ordinary fans. Further, a friction disk fan could be designed to handle fluids of unusual densities and viscosities.

Several other factors should be considered when selecting a fan of this type. Experience with the experimental rotor indicates that the initial cost may be relatively low and that elaborate tools and machinery are not necessary for its construction. The optimum disk spacing decreases with the square root of the speed, thus the manufacturing tolerance on the distance between the disks will limit the maximum speed of the fan. Also the maximum flow rate is limited by the inlet velocity and the physical size of the unit.

Areas of further study should include the determination of the effect of inlet velocity and physical size on the efficiency of the fan. The efficiency of conventional fans increases somewhat as they are made larger.

BIBLIOGRAPHY

1. Beans, Elroy W., Performance Characteristics of a Friction Disk Turbine. Ph.D. Pensylvania State University, 1961.

2. Breiter, M. C. and K. Pohlhausen. Laminar Flow Between Two Parallel Rotating Disks. Aeronautical Research Laboratories, Wright-Patterson AFB, Ohio. Report No. ARL 62-318, 1962.

3. de Kovats, A. and G. Desmur. Pumps, Fans and Compressors. Blackie and Son, Ltd. Glasgow, 1958.

4. Engineering News. Vol. 66, No. 15. October 12, 1911.

5. Flow Measurement. Supplement to ASME Power Test Codes. Chapter 4, Part 5. American Society of Mechanical Engineers, New York, 1959.

6. Hasinger, S. H. and L. G. Kehrt. Investigation of a Shear-Force Pump. JOURNAL OF ENGINEERING FOR POWER, Series A, Transactions of the A.S.M.E., Page 201. July, 1963.

7. Rice, Warren. An Analytical and Experimental Investigation of Multiple Disk Pumps and Compressors. JOURNAL OF ENGINEERING FOR POWER, Series A, Transactions of the A.S.M.E., Page 191, July, 1963.

8. Scientific American, The. September 30, 1911.

9. Shigley, J. E. Machine Design. McGraw-Hill Book Co., Inc. New York, 1956

10. Technical World Magazine. Vol. 16. February, 1912.

11. Wallis, R. A. Axial Flow Fans. Academic Press, Inc. New York, 1961.

APPENDIX A

TYPICAL DATA AND CALCULATIONS FROM THE TEST ROTOR

This section will demonstrate the calculations which were necessary to determine the rotor performance and efficiency.

The flow rate, Q, is found from the pressure drop in the 0.5 inch diameter flow nozzle as follows:

$$Q = \frac{C_v A_2}{\sqrt{1 - \left(\frac{A_2}{A_1}\right)^2}} \sqrt{\frac{2}{\rho}(P_1 - P_2)}$$

The flow coefficient was taken to be 0.94 [5], and because of the nozzle configuration the area A_1 was assumed to be infinity. The flow rate was then given by

$$Q = .226 \sqrt{\frac{\Delta P}{\rho}}$$

The dimensionless radial velocity, pressure and efficiency were determined from the following equations.

$$\bar{U}_o = \frac{Q}{2\pi S \omega r_i^2 (n-1)} \qquad \bar{P} = \frac{P}{\rho \omega^2 r_i^2}$$

$$\eta_R = \frac{Q(P_s + P_d)}{HP}$$

TABLE I

DISK FAN DATA

DISK SIZE 5.2" x 1.7"

NO. OF DISKS 6

SPACING 0.025"

SPEED 2000 RPM

DATE 2-8-64

BAROMETER 29.02 In. Hg.

TEMP. 75°F.

POWER REQUIREMENT

FLOW ΔP	AMPS.	VOLTS
.161	.408	2.90
.150	.403	2.92
.119	.392	2.92
.089	.392	2.82
.069	.367	2.80
.036	.346	2.70
0	.305	2.52

PERFORMANCE TEST

FLOW ΔP	P_s IN.- H_2O
.166	.10
.150	.11
.130	.12
.095	.15
.070	.165
.039	.20
0	.302

TOTAL PRESSURE

FLOW ΔP	P_s IN.- H_2O	P_d IN. - H_2O				
		Disk 1	2	3	4	5
.139	.115	.145	.185	.200	.200	.160
.115	.135	.140	.180	.200	.200	.150
.083	.155	.140	.170	.195	.185	.150
.037	.205	.135	.160	.170	.170	.140
0	.300	.110	.120	.120	.115	.120

It was necessary to run three separate tests to obtain the proper data. These tests are shown in the sample data sheet, Table I. The tests determined the power requirements, the rotor performance and the total pressure rise. The latter test was necessary to determine the efficiency and it was also used to draw Fig. 14 in the text.

The power requirement was determined from the test data by plotting power versus flow rate. This is shown in Table II and Fig. 17.

TABLE II

FAN POWER REQUIREMENT

FLOW CFM	HP x 10^3
1.92	1.590
1.85	1.575
1.65	1.535
1.42	1.480
1.26	1.375
0.95	1.250
0	1.030

From Fig. 17 it is apparent that the friction losses in the system amounted to exactly 1.0 x 10^{-3} HP for this test. The power required by the rotor is found by subtracting this amount from the curve shown.

The performance curve can be drawn by calculating $\bar{P}$ and $\bar{U}_o$ from the data in Table I. This is shown in Table III.

The rotor efficiency is determined from the sum of the average dynamic pressure and the static pressure as shown in Table IV.

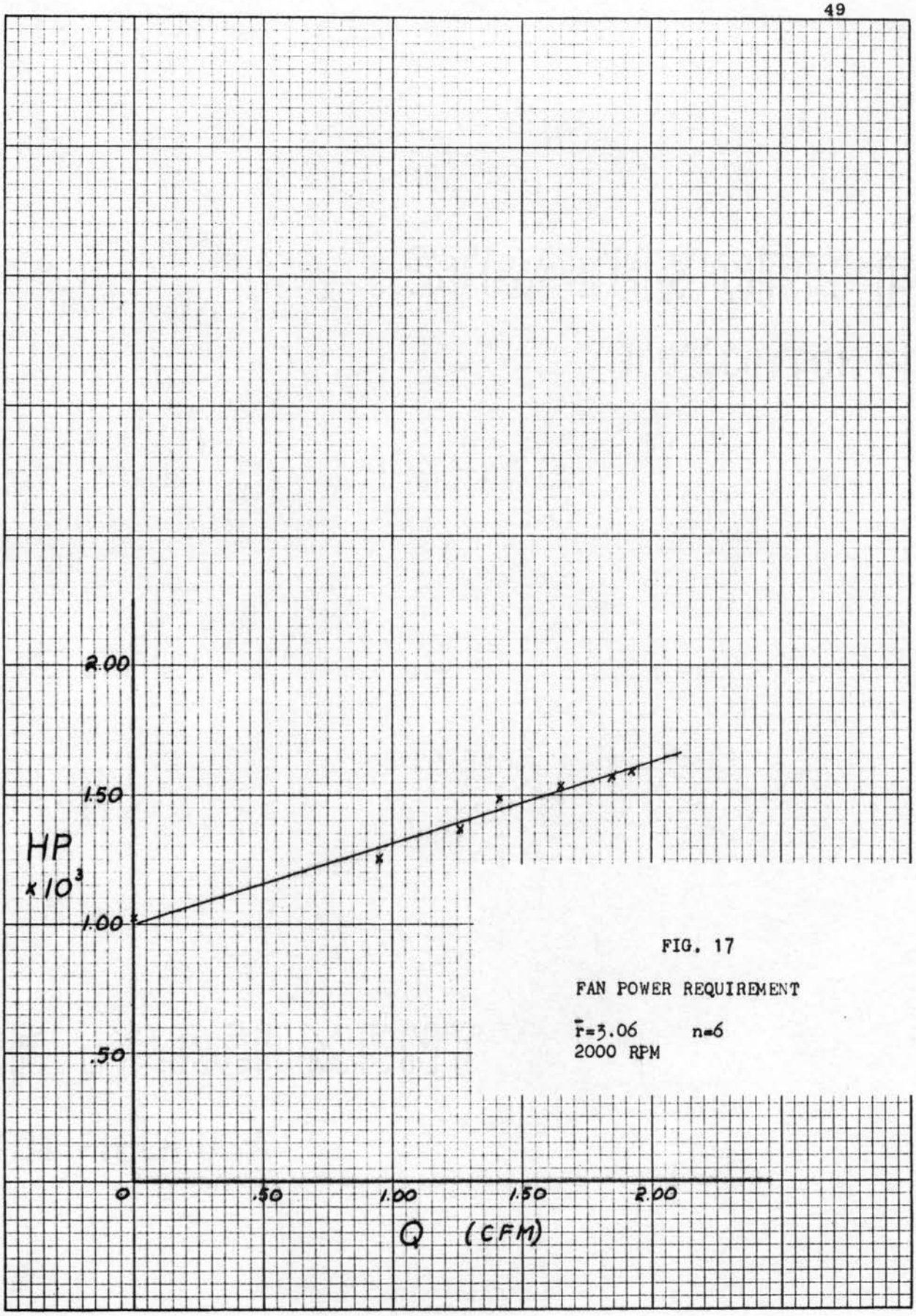

FIG. 17

FAN POWER REQUIREMENT

$\bar{r}$=3.06 n=6
2000 RPM

TABLE III

ROTOR PERFORMANCE

FLOW CFM	$\bar{U}_o$	P_s IN.- H_2O	$\bar{P}$
1.95	.471	.10	1.05
1.85	.447	.11	1.16
1.72	.415	.12	1.265
1.47	.355	.15	1.58
1.265	.306	.165	1.74
0.942	.228	.20	2.11
0	0	.302	3.18

TABLE IV

ROTOR EFFICIENCY

FLOW CFM	P_s IN.- H_2O	P_d (Avg.) IN.- H_2O	AVG. TOTAL PRESSURE	HP x 10^3	η_R
1.78	.115	.178	.293	.560	14.6
1.62	.135	.174	.309	.500	15.8
1.38	.155	.168	.323	.430	16.3
.92	.205	.155	.360	.280	18.6

APPENDIX B

CALCULATION OF EFFECT OF VELOCITY CHANGES IN THE INLET REGION ON THE PRESSURE MEASUREMENTS

The mathematical analysis is concerned with the pressure at station (2), Fig. 18. It is desirable therefore to calculate the magnitude of the error introduced by measuring this pressure at station (1). When the fluid enters the disk section (station 2) it has both radial and tangential components of velocity. The velocity here is not the same as that at station (1).

Bernoulli's equation applied to this system shows that

$$P_1 + \frac{\rho}{2} W_1^2 = P_2 + \frac{\rho}{2} [U_2^2 + V_2^2]$$

$$P_1 - P_2 = \frac{\rho}{2} [U_2^2 - W_1 + V_2^2] \qquad (B-1)$$

The mathematical analysis assumed an initial radial velocity of $\bar{v}_o$, thus

$$U_2 = U_o = \bar{U}_o \omega r_i$$

The axial inlet velocity W_1 can be expressed by

$$W_1 = \frac{Q}{\pi r_i^2} = \frac{4\pi d r_i^2 \omega \bar{U}_o (n-1)}{\pi r_i^2}$$

Thus,

$$W_1 = 4 d \omega \bar{U}_o (n-1)$$

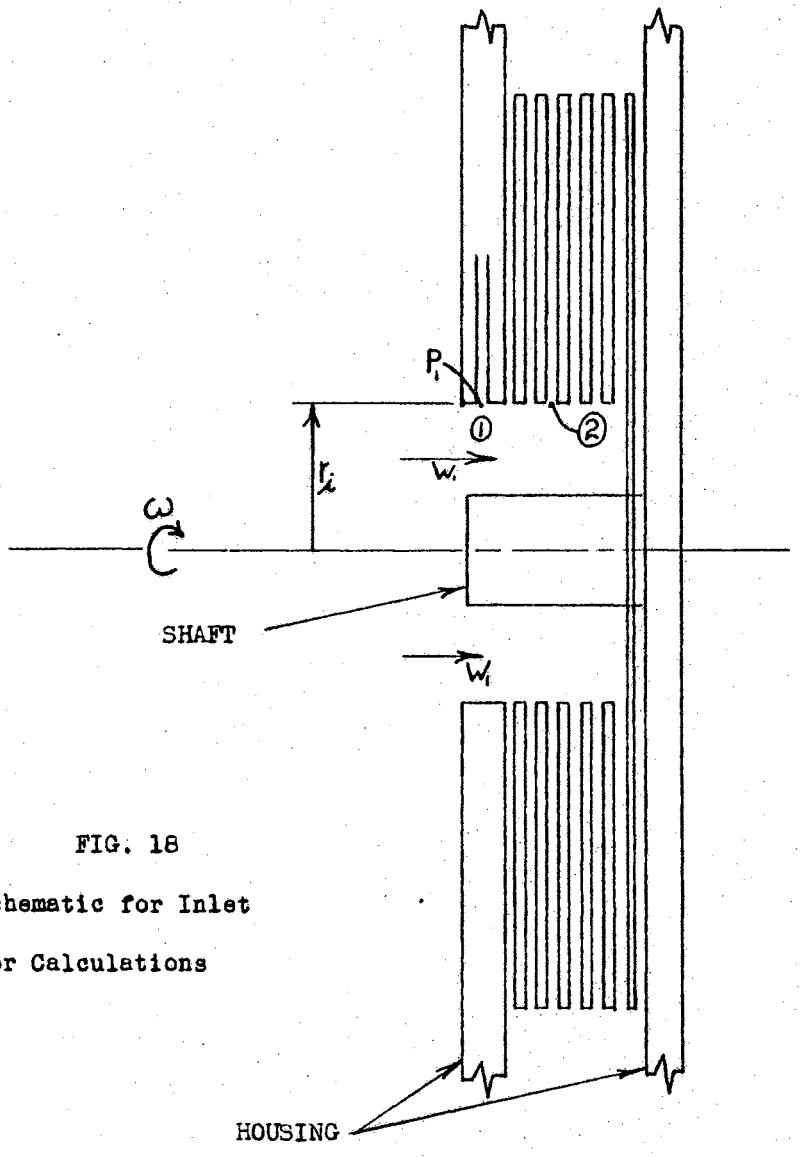

FIG. 18

Schematic for Inlet

Error Calculations

The initial tangential velocity V was assumed to be zero but for the purpose of this discussion we must use its maximum possible value. This maximum will occur when the fluid tangential velocity is equal to that of the disks at the inlet, thus

$$V_2 = \omega r_i.$$

Substituting these relationships into equation (B-1) gives

$$P_1 - P_2 = \frac{\rho}{2}\left[\bar{U}_o^2 \omega^2 r_i^2 - (4d\omega \bar{U}_o (n-1))^2 + \omega^2 r_i^2\right]$$

This equation can be simplified by using the dimensionless pressure

$$\bar{P}_1 - \bar{P}_2 = \frac{P_1 - P_2}{\rho \omega^2 r_i^2} = \frac{\bar{U}_o^2}{2} - \frac{8d^2 \bar{U}_o^2 (n-1)^2}{r_i^2} + \frac{1}{2} \qquad (B-2)$$

The magnitude of the error can now be calculated from typical test fan conditions as follows, $\bar{U}_o = 0.5$, d = 0.0125 inches, n = 6, r_i = 0.85 inches.

From this data we find that

$$\bar{P}_1 - \bar{P}_2 = 0.125 - 0.0108 + 0.5$$

In the test fan the effect of the axial inlet velocity was assumed to be small so that it could be neglected. The calculated error of 0.0108 indicates that this assumption was permissible.

The error of 0.125 contributed by the radial velocity increase is close to the limit of accuracy of the test equipment.

The last term is due to the assumed increase in tangential velocity. It can be seen that a significant error could occur in the test data at this point.

VITA

Dixon Keith Foss

Candidate for the Degree of

Master of Science

Thesis: DESIGN ANALYSIS OF A FRICTION DISK ROTOR

Major Field: Mechanical Engineering

Biographical:

Personal Data: Born in Long Beach, California, February 7, 1941, the son of Edwin and Lorene Foss.

Education: Graduated from Edison High School Tulsa, Oklahoma, in 1958 and the following September entered Rose Polytechnic Institute; transferred to Oklahoma State University in January, 1960, and received Bachelor of Science degree in Mechanical Engineering in 1962; completed requirements for Master of Science degree in August, 1964.

Professional experience: Employed by National Science Foundation Plasma Research Facility; served on this project as undergraduate and graduate assistant for two years.